ELIMINATION OF UNBALANCE VIBRATION IN AMB SYSTEMS USING GAIN SCHEDULED H_∞ ROBUST CONTROLLERS

Fumio Matsumura
Department of Electrical and Computer Engineering, Kanazawa University, Kanazawa, Ishikawa, Japan
Masayuki Fujita
School of Information Science, Japan Advanced Institute of Science and Technology, Hokuriku, Tatsunokuchi, Ishikawa, Japan
Kazuhiro Hatake
Basic Engineering Research Group, Research Division, Komatsu Ltd., Hiratsuka, Kanagawa, Japan
Masatoshi Hirai
Department of Electrical and Computer Engineering, Kanazawa University, Kanazawa, Ishikawa, Japan

ABSTRACT
This paper deals with the problem of an unbalance vibration in AMB (Active Magnetic Bearing) systems. We design a control system achieving the elimination of the unbalance vibration, using a Loop Shaping Design Procedure (LSDP). After the introduction of our experimental setup, a mathematical model of the magnetic bearing is shown. Then, the gain scheduled H_∞ robust controller is designed, based on the LSDP, so as to reject the disturbances caused by unbalance on the rotor asymptotically even if the rotational speed of the rotor varies. Finally, with simulation results, we show that such a control is possible by using the designed controller.

INTRODUCTION
When the rotor supported by magnetic bearings rotates, various serious problems arise. In this paper, among such problems, we focus on both the problem of the vibration caused by unbalance on the rotor and the problem of the interference caused by gyroscopic effect.

We already have designed the controllers, in consideration of the above problems, using the Loop Shaping Design Procedure (LSDP) proposed by McFarlane and Glover [1], and have experimentally demonstrated their availability for the elimination of the unbalance vibration [2]. However, it was achieved at the regular rotational speed of the rotor, and it is naturally required that the controllers achieve the elimination of the unbalance vibration even if the rotational speed of the rotor varies. Hence, in this paper, we introduce the gain scheduled controller by scheduling the free parameter as a function of rotational speed of the rotor. We therefore show the conditions whereby, using LSDP, we can get the controllers that achieve asymptotic disturbance rejection and robust stability. Finally, we present the results of simulations with the scheduled controllers.

EXPERIMENTAL SETUP
The AMB system used in this work is a 4-axis controlled horizontal shaft magnetic bearing with symmetric structure. An outline of the setup is depicted in Figure 1. Physical parameters of this experimental machine are shown in Table 1.

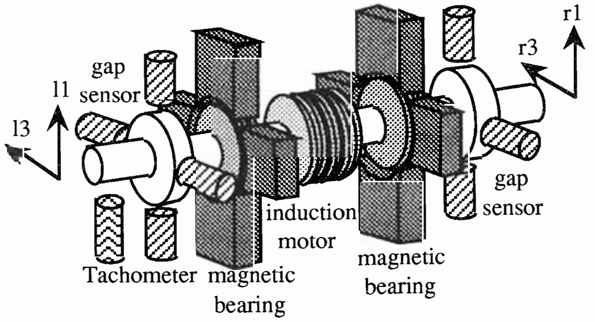

FIGURE 1. DIAGRAM OF EXPERIMENTAL MACHINE

TABLE 1. PARAMETER OF THE AMB SYSTEM

Parameter	Symbol	Value	Unit
Mass of the Rotor	m	1.39×10^{1}	kg
Moment of Inertia about X	J_x	1.348×10^{-2}	kg·m²
Moment of Inertia about Y	J_y	2.326×10^{-1}	kg·m²
Distance between Center of Mass and Electromagnet	$l_{l,r}$	1.30×10^{-1}	m
Steady Gap	W	5.5×10^{-4}	m
Steady Attractive Force	$F_{l2\sim4,r2\sim4}$	9.09×10	N
	$F_{l1,r1}$	2.20×10	N
Steady Current	$I_{l2\sim4,r2\sim4}$	6.3×10^{-1}	A
	$I_{l1,r1}$	3.1×10^{-1}	A
Resistance	R	1.07×10	Ω
Inductance	L	2.85×10^{-1}	H

MODELING OF MAGNETIC BEARING

A mathematical model of the magnetic bearing has been derived in [3] is given by

$$\begin{bmatrix} \dot{x}_v \\ \dot{x}_h \end{bmatrix} = \begin{bmatrix} A_v & pA_{vh} \\ pA_{hv} & A_h \end{bmatrix} \begin{bmatrix} x_v \\ x_h \end{bmatrix} + \begin{bmatrix} B_v & 0 \\ 0 & B_h \end{bmatrix} \begin{bmatrix} u_v \\ u_h \end{bmatrix} \quad (1)$$

$$\begin{bmatrix} y_v \\ y_h \end{bmatrix} = \begin{bmatrix} C_v & 0 \\ 0 & C_h \end{bmatrix} \begin{bmatrix} x_v \\ x_h \end{bmatrix} \quad (2)$$

where the subscripts '*v*' and '*h*' in the vectors and the matrices stand for the vertical motion and the horizontal motion of the magnetic bearing, respectively. In addition, the subscripts '*vh*' and '*hv*' stand for the interference term between the vertical motion and horizontal motion, and *p* denotes the rotational speed on the rotor.

Each vector in (1) and (2) is defined as

$$x_v = \begin{bmatrix} g_{l1} & g_{r1} & \dot{g}_{l1} & \dot{g}_{r1} & i_{l1} & i_{r1} \end{bmatrix}^T \quad (3)$$

$$x_h = \begin{bmatrix} g_{l3} & g_{r3} & \dot{g}_{l3} & \dot{g}_{r3} & i_{l3} & i_{r3} \end{bmatrix}^T \quad (4)$$

$$u_v = \begin{bmatrix} e_{l1} & e_{r1} \end{bmatrix}^T, \quad u_h = \begin{bmatrix} e_{l3} & e_{r3} \end{bmatrix}^T \quad (5)$$

where

g_j : deviations from the steady gap lengths between the electromagnets and the rotor

i_j : deviations from the steady currents of the electromagnets

e_j : deviations from the steady voltages of the electromagnets

$j = l1, r1, l3, r3$.

The subscripts '*l*' and '*r*' denote the left-hand side and the right-hand side of the magnetic bearing respectively, and the subscripts '1' and '3' denote one of the vertical directions and one of the horizontal directions of the rotor respectively.

Each matrix in (1) and (2) is as follows.

$$A_v = \begin{bmatrix} 0 & 0 & 1 & 0 & 0 & 0 \\ 0 & 0 & 0 & 1 & 0 & 0 \\ 5.937e4 & -2.933e2 & 0 & 0 & -6.225e1 & 3.076e-1 \\ -2.933e2 & 5.937e4 & 0 & 0 & 3.076e-1 & -6.225e1 \\ 0 & 0 & 0 & 0 & -3.754e1 & 0 \\ 0 & 0 & 0 & 0 & 0 & -3.754e1 \end{bmatrix}$$

$$A_h = \begin{bmatrix} 0 & 0 & 1 & 0 & 0 & 0 \\ 0 & 0 & 0 & 1 & 0 & 0 \\ 2.314e4 & -1.143e2 & 0 & 0 & -4.105e1 & 2.028e-1 \\ -1.143e2 & 2.314e4 & 0 & 0 & 2.028e-1 & -4.105e1 \\ 0 & 0 & 0 & 0 & -3.754e1 & 0 \\ 0 & 0 & 0 & 0 & 0 & -3.754e1 \end{bmatrix}$$

$$A_{vh} = -A_{hv} = \begin{bmatrix} 0 & 0 & 0 & 0 & 0 & 0 \\ 0 & 0 & 0 & 0 & 0 & 0 \\ 0 & 0 & -3.034e-3 & 3.034e-3 & 0 & 0 \\ 0 & 0 & 3.034e-3 & -3.034e-3 & 0 & 0 \\ 0 & 0 & 0 & 0 & 0 & 0 \\ 0 & 0 & 0 & 0 & 0 & 0 \end{bmatrix}$$

$$B_v = B_h = \begin{bmatrix} 0 & 0 \\ 0 & 0 \\ 0 & 0 \\ 0 & 0 \\ 3.509 & 0 \\ 0 & 3.509 \end{bmatrix}$$

$$C_v = C_h = \begin{bmatrix} 1 & 0 & 0 & 0 & 0 & 0 \\ 0 & 1 & 0 & 0 & 0 & 0 \end{bmatrix}$$

GAIN SCHEDULED H_∞ CONTROLLER

Let (*N*, *M*) represent a normalized left coprime factorization of a plant *G*. Let these coprime factors be assumed to have uncertainties Δ_N, Δ_M and let G_Δ represent the plant with these uncertainties.

$$G_\Delta = M_\Delta^{-1} N_\Delta = (M + \Delta_M)^{-1}(N + \Delta_N) \quad (6)$$

where N_Δ and M_Δ represent a left coprime factorization of G_Δ, and

$$\Delta = \left\{ \begin{bmatrix} \Delta_N, & \Delta_M \end{bmatrix} \in RH_\infty ; \left\| \begin{bmatrix} \Delta_N, & \Delta_M \end{bmatrix} \right\|_\infty < \varepsilon \right\} . \quad (7)$$

G_Δ can be written in a form of an Upper Linear Fractional Transformation (ULFT) as follows.

$$G_\Delta = F_U(P, \Delta) = P_{22} + P_{21}\Delta(I - P_{11}\Delta)^{-1} P_{12} \quad (8)$$

where

$$P = \left[\begin{array}{c|c} P_{11} & P_{12} \\ \hline P_{21} & P_{22} \end{array} \right] = \left[\begin{array}{c|c} 0 & I \\ \hline M^{-1} & G \\ M^{-1} & G \end{array} \right] . \quad (9)$$

The robust stabilization problem for the uncertain plant in (6) can be treated as the next H_∞ control problem:

$$\left\| \begin{bmatrix} K \\ I \end{bmatrix} (I - GK)^{-1} M^{-1} \right\|_\infty \le \varepsilon^{-1} := \gamma . \quad (10)$$

It is known that the solution of this problem and the largest number of ε ($= \varepsilon_{\max} := \gamma_{\min}$) can be obtained by solving two Riccati equations without iterative procedure. All controllers *K* satisfying (10) are given by

$$K = F_L(K_a, \Phi) := K_{11} + K_{12}\Phi(I - K_{22}\Phi)^{-1} K_{21} \quad (11)$$

where

$$K_a = \begin{bmatrix} K_{11} & K_{12} \\ K_{21} & K_{22} \end{bmatrix} \quad (12)$$

$$\Phi \in RH_\infty \text{ with } \|\Phi\|_\infty \le 1 . \quad (13)$$

For the calculation of K_a and $\varepsilon_{\max}$, see [1].
In order to eliminate the unbalance vibration of the rotor, which can be modeled as sinusoidal disturbances [4], the robust controller should be designed to achieve sinusoidal disturbance rejection asymptotically. In this case, as is well known, the controller must have the imaginary poles at the frequencies corresponding to the rotational speed of the rotor [5]. Hence, when we consider the rejection of sinusoidal disturbance whose frequency is ω_0 (rad/s), $K(s)$ is required to satisfy

$$K(\pm j\omega_0) = \infty \Leftrightarrow \{I - G(\pm j\omega_0)K(\pm j\omega_0)\}^{-1} = 0 . \quad (14)$$

We then derive the conditions, by adopting the H_∞ problem with boundary constraints [6] shown in Appendix to this problem, whereby there exist the controllers satisfying both (10) and (14). The boundary constraint $\{L, \Pi, \Psi\}$ corresponding to (14) is given by

$$L = [0 \quad I] , \quad \Pi = M(\pm j\omega_0) , \quad \Psi = 0 . \quad (15)$$

The basic constraint $\{L_B, \Psi_B\}$ in (35) is described by

$$L_B = P_{12}^{\perp}(\pm j\omega_0) = [-G(\pm j\omega_0) \quad I] , \quad (16)$$

$$\Psi_B = P_{12}^{\perp}(\pm j\omega_0)P_{11}(\pm j\omega_0) = M^{-1}(\pm j\omega_0) . \quad (17)$$

It is obvious that $\{L, \Pi, \Psi\}$ is satisfying condition (b) of Theorem A., and the extended boundary constraint $\{\hat{L}, \hat{\Psi}\}$ in (36) is given by

$$\hat{L} = \begin{bmatrix} -G(\pm j\omega_0) & I \\ 0 & I \end{bmatrix} , \quad \hat{\Psi} = \begin{bmatrix} I \\ 0 \end{bmatrix} . \quad (18)$$

After some straightforward calculation, we have

$$\gamma\overline{\sigma}\left(N(\pm j\omega_0)\right) > 1 \quad (19)$$

where

$$\overline{\sigma}\left(N(\pm j\omega_0)\right) = \left(\frac{\overline{\sigma}^2\left(G(\pm j\omega_0)\right)}{1 + \overline{\sigma}^2\left(G(\pm j\omega_0)\right)} \right)^{1/2}$$

$\overline{\sigma}(\bullet)$: the maximum singular value

from the condition (c) of Theorem A.
If we choose free parameter $\Phi(s)$ such that

$$\Phi(\pm j\omega_0) = K_{22}^{-1}(\pm j\omega_0) \quad (20)$$

under the conditions (13) (19), it can be seen that we obtain the controller with the imaginary poles at $\pm j\omega_0$ from (11).
Based on the above, we design the control system using the Loop Shaping Design Procedure (LSDP) [1]. The procedure is briefly outlined below:

<Step 1> Loop Shaping

Selecting shaping function W_1 and W_2, the singular values of the nominal plant G are shaped to have a desired open loop shape. Let G_s represent this shaped plant

$$G_s = W_2 G W_1 . \quad (21)$$

W_1 and W_2 should be selected such that G_s has no hidden unstable modes.

<Step 2> Robust Stabilization

The maximum stability margin $\varepsilon_{\max}$ is calculated. If $\varepsilon_{\max} << 1$, return to step 1, then W_1 and W_2 should be selected again. Otherwise, γ is appropriately selected as $\gamma \ge \gamma_{\min} = \varepsilon_{\max}$ and K_a is calculated. The free parameter Φ is selected such as (20) under the conditions, then the H_∞ controller K_∞ is synthesized for G_s from (11).

<Step 3> Final Controller

The final controller K can be obtained by the combination of W_1, W_2 and K_∞

$$K = W_1 K_\infty W_2 . \quad (22)$$

In this procedure, $\varepsilon_{\max}$ is treated as a design indicator rather than the maximum stability margin of G_s.
Thus, we can design the robust controllers achieving sinusoidal disturbance rejection asymptotically using the LSDP. Moreover, utilizing the free parameter for such design, it is possible to obtain the gain scheduled controllers by scheduling the free parameter as the function of rotational speed of the rotor, which achieve the elimination of the unbalance vibration even if the rotational speed of the rotor varies.

CONTROLLER DESIGN

In this section, the feedback controllers are designed with the LSDP. We assume rotational speed $p = 0$ in the nominal plant G. In this case, from (1), we see that there is no coupling between the vertical motion and horizontal motion. Therefore, the plant model can be separated into the vertical plant $G_v(s) := C_v(sI - A_v)^{-1}B_v$ and the horizontal plant $G_h(s) := C_h(sI - A_h)^{-1}B_h$, respectively.

$$G = \begin{bmatrix} G_v & 0 \\ 0 & G_h \end{bmatrix} \quad (23)$$

Then, two controllers will be designed for the each plant, respectively. The final controller K for the entire plant G will be constructed with the combination of these controllers.

$$K = \begin{bmatrix} K_v & 0 \\ 0 & K_h \end{bmatrix} \tag{24}$$

where K_v denotes the controller for the vertical plant, and K_h denotes the controller for the horizontal plant. The shaping functions and the design parameters are selected as follows.

(v) Design for vertical motion

$$W_{1v}(s) = \frac{1300(1+s/(2\pi\cdot 5))(1+s/(2\pi\cdot 35))}{(1+s/(2\pi\cdot 0.01)(1+s/(2\pi\cdot 700))} \times \frac{(1+s/(2\pi\cdot 50))}{(1+s/(2\pi\cdot 1200))}\begin{bmatrix} 1 & 0 \\ 0 & 1 \end{bmatrix} \tag{25}$$

$$W_{2v}(s) = 10000\begin{bmatrix} 1 & 0 \\ 0 & 1 \end{bmatrix} \tag{26}$$

$$\varepsilon_{\max v} = 0.19944\ , \quad \varepsilon_v^{-1} = \gamma_v = 5.25 \tag{27}$$

(h) Design for horizontal motion

$$W_{1h}(s) = \frac{1100(1+s/(2\pi\cdot 5))(1+s/(2\pi\cdot 25))}{(1+s/(2\pi\cdot 0.01)(1+s/(2\pi\cdot 700))} \times \frac{(1+s/(2\pi\cdot 40))}{(1+s/(2\pi\cdot 1200))}\begin{bmatrix} 1 & 0 \\ 0 & 1 \end{bmatrix} \tag{28}$$

$$W_{2h}(s) = 10000\begin{bmatrix} 1 & 0 \\ 0 & 1 \end{bmatrix} \tag{29}$$

$$\varepsilon_{\max h} = 0.27432\ , \quad \varepsilon_h^{-1} = \gamma_h = 3.75\ . \tag{30}$$

In this design, verifying the condition (19), it can be seen that it is possible to design the controllers below ω_0= 324.63 rad/s (p = 3100 rpm) from Figure 2. In order to satisfy the conditions (13) and (20), within the above limits, the free parameters are selected as

$$\Phi_d(s) = \begin{bmatrix} C_{\Phi 1d} & C_{\Phi 2d} \end{bmatrix}(sI - A_{\Phi d})^{-1}B_{\Phi d} \tag{31}$$

where

$$A_{\Phi d} = \begin{bmatrix} -a_d & 0 \\ 0 & -b_d \end{bmatrix},\quad B_{\Phi d} = \begin{bmatrix} I \\ I \end{bmatrix}$$

$$C_{\Phi 1d} = \frac{(a_d^2+\omega_0^2)}{\omega_0(a_d-b_d)}\left\{\omega_0 \operatorname{Re}(K_{22d}^{-1}(j\omega_0)) + b_d \operatorname{Im}(K_{22d}^{-1}(j\omega_0))\right\}$$

$$C_{\Phi 2d} = \frac{(b_d^2+\omega_0^2)}{\omega_0(b_d-a_d)}\left\{\omega_0 \operatorname{Re}(K_{22d}^{-1}(j\omega_0)) + a_d \operatorname{Im}(K_{22d}^{-1}(j\omega_0))\right\}$$

with

$$a_d = 2\pi\omega_0/60\ ,\quad b_d = 0.012a_d - 0.2\quad (d = v, r\ ).$$

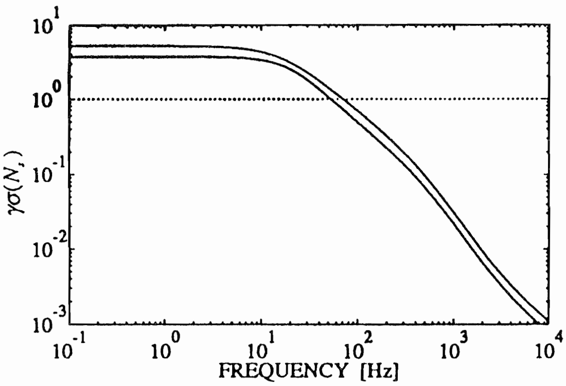

FIGURE 2 $\gamma\sigma(N_s)$

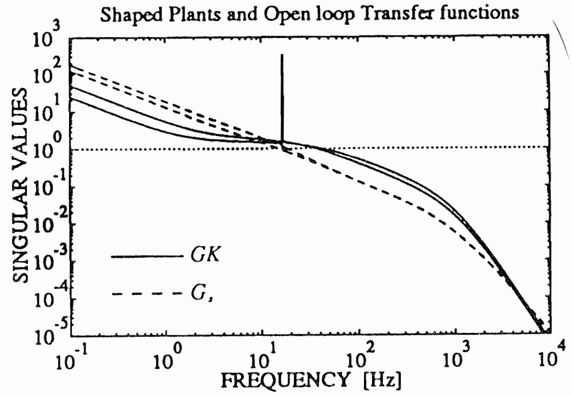

FIGURE 3 SHAPED PLANTS AND OPEN LOOP TRANSFER FUNCTIONS

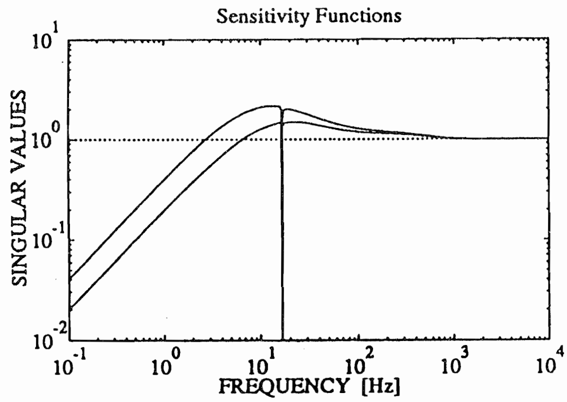

FIGURE 4 $\sigma((I-GK)^{-1})$

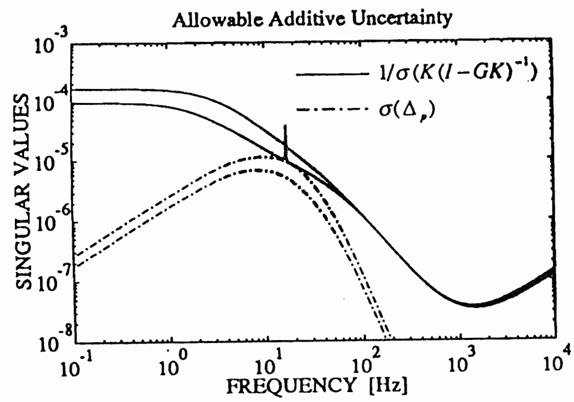

FIGURE 5 $1/\sigma(K(I-GK)^{-1})$ AND $\sigma(\Delta_p)$

When we obtain the shaped plants, a model reduction technique has been employed. The procedure of the model reduction is 'The Nominal Plant Model Reduction Procedure' as shown in [1, Procedure 5.5]. The order of the each shaped plant has been reduced from 12 states to 8. As a consequence, the final controller has 36 states. As a example, we design the control system with $\omega_0 = 104.72$ rad/s (p = 1000 rpm). The singular values of the shaped plants and the open loop transfer functions are shown in Figure 3. Figure 4 shows the singular values of the sensitivity functions. From the figure, we can see that sensitivity approaches zero at the frequency ω_0.
In this design, we ignored the interference terms, which express the gyroscopic effect, as $p = 0$. We therefore verify the robust stability of this system against changes in the rotational speed of the rotor. Let the perturbed plant ($p \neq 0$) be denoted by G_p and the additive perturbation Δ_p of G_p from G is as follows:

$$\Delta_p = G_p - G \ . \tag{32}$$

In Figure 5, the singular values $1/\sigma(K(I-GK)^{-1})$ and $\sigma(\Delta_p)$ at $\omega_0 = 1675.5$ rad/s (p = 16000 rpm) are shown. This system is stable at $\omega_0 \leq 1675.5$ rad/s, because $\bar{\sigma}(\Delta_p)$ is smaller than the allowable additive uncertainty $1/\bar{\sigma}(K(I-GK)^{-1})$ at all frequencies.

SIMULATION RESULTS

The simulations are carried out by using SIMULINK. The following figures show the displacement on the left side of the rotor when the rotational speed is varied at the rate of 2 rpm a second. The results with the controller designed at 1000 rpm when the rotational speed is varied from 900 rpm to 1100 rpm are shown in Figure 6. The results with the controller designed at 3000 rpm when the rotational speed is varied from 2900 rpm to 3100 rpm are shown in Figure 7. Similarly, the results with the gain scheduled controllers are shown in Figure 8 and Figure 9, respectively. From these results, it can be seen that even if the rotational speed of the rotor varies, the elimination of the unbalance vibration of the rotor can be achieved by the gain scheduled H_∞ controllers.

CONCLUSION

In this paper, we introduced gain scheduled H_∞ robust controllers by scheduling the free parameter as the function of rotational speed of the rotor, in order to eliminate the unbalance vibration even if the rotational speed of the rotor varies. For such a design, we employed the LSDP. Moreover, we showed the conditions whereby we can get such controllers. Finally, results of the simulations showed the availability of the gain scheduled H_∞ robust controllers designed for the elimination of the unbalance vibration at the variable rotational speed of the rotor.

APPENDIX

Definition A. "H_∞ problem with boundary constraints"

Find the $K(s)$ satisfying

(s1) $K(s)$ stabilizes $F_U(P,0)$,

$$\text{(s2)}\ \|P_{zw}\|_\infty \leq \varepsilon^{-1} := \gamma \ , \tag{33}$$

$$\text{(s3)}\ LP_{zw}(j\omega)\Pi = \Psi \ , \tag{34}$$

where $P_{zw} := F_L(P,K)$.

Definition B. "Basic constraints"

$$L_B := P_{12}^{\perp}(j\omega) \ , \ \ \Psi_B := P_{12}^{\perp}(j\omega)P_{11}(j\omega) \ , \tag{35}$$

where $P_{12}^{\perp}(s)P_{12}(s) = 0$.

Definition C. "Extended constraints"

$$\hat{L} := \begin{bmatrix} L_B \\ L \end{bmatrix}, \ \ \hat{\Psi} := \begin{bmatrix} \Psi_B \Pi \\ \Psi \end{bmatrix}, \tag{36}$$

where $\hat{L}$ and $\hat{\Psi}$ are row full rank.

Theorem A.

H_∞ problem with boundary constraints $\{L, \Pi, \Psi\}$ is solvable, iff the following three conditions hold:

(a) The H_∞ problem is solvable.

$$\text{(b)}\ rank\begin{bmatrix} L_B & \Psi_B \Pi \\ L & \Psi \end{bmatrix} = rank\begin{bmatrix} L_B \\ L \end{bmatrix}. \tag{37}$$

$$\text{(c)}\ \hat{L}\hat{L}^* > \gamma^2 \hat{\Psi}(\Pi^*\Pi)^{-1}\hat{\Psi}^* . \tag{38}$$

REFERENCES

[1] D. McFarlane and K. Glover, Robust Controller Design Using Normalized Coprime Factor Plant Descriptions, *Lecture Notes in Control and Information Sciences*, 138, Springer-Verlag, 1990.

[2] M. Fujita, K. Hatake, F. Matsumura and K. Uchida, "Experiments on the Loop Shaping Based H_∞ Control of a Magnetic Bearing," *Proc. of 1993 ACC*, San Francisco, California, pp. 8-12, 1993.

[3] F. Matsumura, H. Kobayashi and Y. Akiyama, "Fundamental Equation of Horizontal Shaft Magnetic Bearing and its Control System Design (in Japanese)," *Trans. IEE of Japan*, vol. 101-C, no. 6, pp. 137-144, 1981; also *Electrical Engineering in Japan*, vol. 101, no. 3, pp. 123-130, 1981.

[4] F. Matsumura, M. Fujita and K. Hatake, "Output Regulation in Magnetic Bearing Systems by a Dynamic Output Feedback Controller (in Japanese)," *T. IEE Japan*, vol. 112-C, no. 10, pp. 977-983, 1992.

[5] T. Sugie, M. Fujita and S. Hara, "Multiobjective Controller Design with the Guaranteed H_∞ Control Performance," *12th IFAC World Congress*, Sydney, Australia, vol. 4, pp. 43-46, 1993.

[6] T. Sugie and S. Hara, "H_∞-suboptimal control problem with boundary constraints," *System & Control Letters*, vol. 13, no. 2, pp. 93-99, 1989.

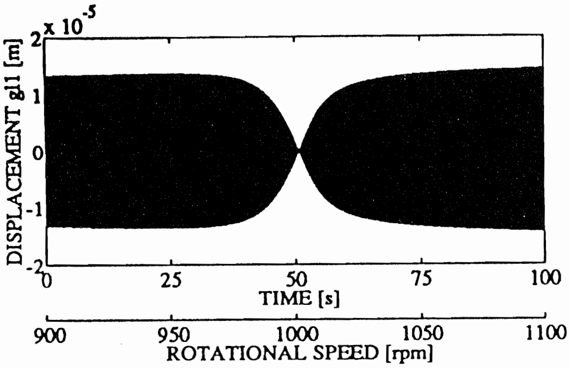

(a) Vertical

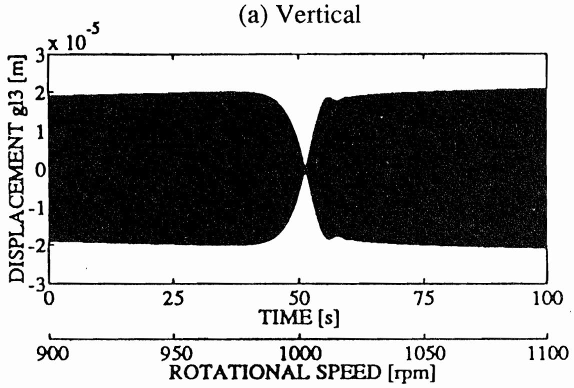

(b) Horizontal

FIGURE 6 CONTROLLER DESIGNED AT 1000 rpm (900 rpm - 1100 rpm)

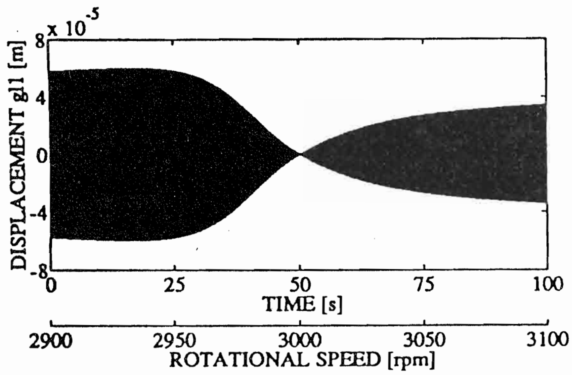

(a) Vertical

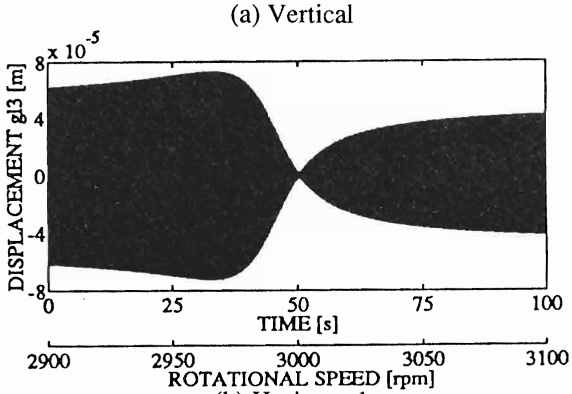

(b) Horizontal

FIGURE 7 CONTROLLER DESIGNED AT 3000 rpm (2900 rpm - 3100 rpm)

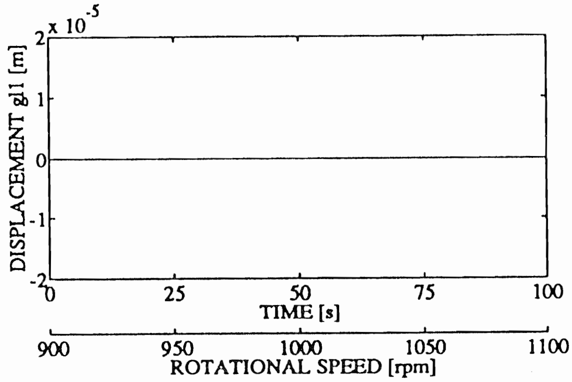

(a) Vertical

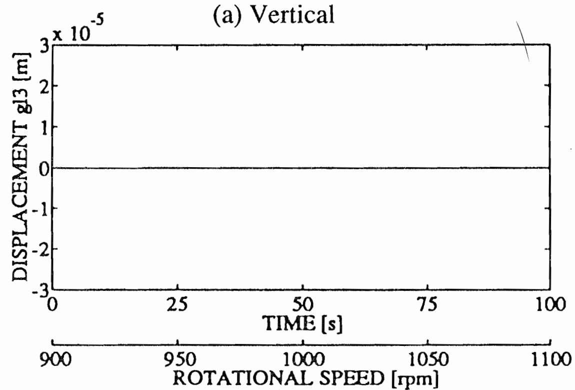

(b) Horizontal

FIGURE 8 GAIN SCHEDULED CONTROLLER (900 rpm - 1100 rpm)

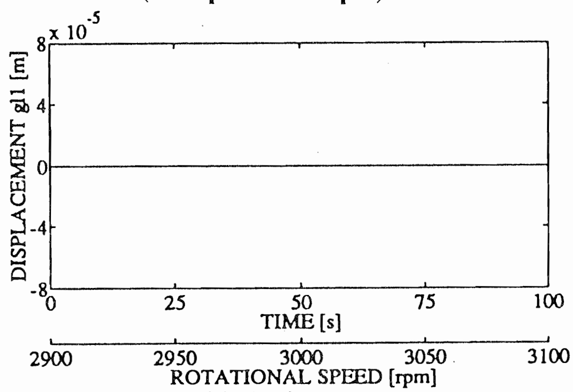

(a) Vertical

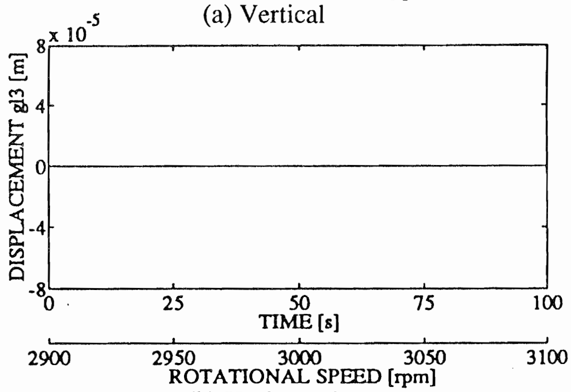

(b) Horizontal

FIGURE 9 GAIN SCHEDULED CONTROLLER (2900 rpm - 3100 rpm)